Selective inhibition of soluble TNF using XPro1595 improves hippocampal pathology to promote improved neurological recovery following traumatic brain injury in mice

Kirsty Dixon (kirsty.dixon@vcuhealth.org)
VCU: Virginia Commonwealth University
Katelyn Larson
Virginia Commonwealth University
Melissa Damon
Virginia Commonwealth University
Rajasa Randhi
Virginia Commonwealth University
Nancy Nixon-Lee
Virginia Commonwealth University

Research Article

Keywords: TNF, TNFR1, inflammation, glial reactivity, synaptic plasticity, learning and memory, depression, neuropathic pain

Posted Date: July 20th, 2021

DOI: https://doi.org/10.21203/rs.3.rs-734211/v1

Title: Selective inhibition of soluble TNF using XPro1595 improves hippocampal pathology to promote improved neurological recovery following traumatic brain injury in mice

Katelyn Larson [a], Melissa Damon [a], Rajasa Randhi [a], Nancy Nixon-Lee, Kirsty J. Dixon *

Department of Surgery, Virginia Commonwealth University, Richmond VA 23298

[a] equal contributors

[*] corresponding author

Running Title: XPro1595 improves TBI outcomes

ABSTRACT

BACKGROUND: Symptoms associated with traumatic brain injury (TBI) can be debilitating, and treatment without off-target side-effects remains a challenge. This study aimed to investigate the efficacy of selectively inhibiting the soluble form of TNF (solTNF) using the biologic XPro1595 in a mouse model of TBI. METHODS: Mild-to-moderate traumatic brain injury (CCI model) was induced in adult male C57Bl/6J mice, with XPro1595 (10 mg/kg, S.C.) or vehicle being administered in a clinically relevant window (60 minutes post-injury). The animals were assessed for differences in neurological function, and hippocampal tissue was analyzed for inflammation and glial reactivity, as well as neuronal degeneration and plasticity. RESULTS: We report that unilateral CCI over the right parietal cortex in mice promoted deficits in learning and memory, depressive-like behavior and neuropathic pain. Using immunohistochemical and Western blotting techniques, we observed the cortical injury promoted a set of expected pathophysiology's within the hippocampus consistent with the observed neurological outcomes, including glial reactivity, enhanced neuronal dendritic degeneration (dendritic beading), and reduced synaptic plasticity (spine density and PSD-95 expression) within the DG and CA1 region of the hippocampus. These effects were prevented in the mice treated with XPro1595. CONCLUSION: Overall, we observed that selectively inhibiting solTNF using XPro1595 improved the pathophysiological and neurological sequelae of brain-injured mice, which provides support of its use in patients with TBI.

Keywords: TNF, TNFR1, inflammation, glial reactivity, synaptic plasticity, learning and memory, depression, neuropathic pain

INTRODUCTION

TBI affects 1.5M people annually in the United States, with approximately 80% being mild TBI, and symptoms range from physical, cognitive, psychological and/or psychosocial impairments. TBI is also a known risk factor for the later development of AD (1). The pathophysiological sequelae of TBI results from an acute and chronic phase of injury characterized by cell death and degeneration and neural

connectome dysfunction/reorganization. In the acute phase, neuronal death is initiated by mechanical forces, which alter cell membrane and vascular integrity, creating a microenvironment susceptible to necrotic and apoptotic processes (2-5). The secondary injury phase occurs within minutes after the onset of TBI whereby the release of pro-inflammatory cytokines mobilizes immune and glial cells to the site of injury causing edema and inflammation (6-11). This phase is also associated with gliosis, demyelination, continued apoptosis and neuronal degeneration/plasticity. Within the damaged brain, the inflammatory response causes a sustained upregulation of cytokines, such as interleukin 1-beta (IL-1β), IL-6 and TNF (12-14), and excess solTNF within the hippocampus activates TNFR1 to promote reductions in dendritic spine density, length, and protein expression (PSD-95, synapsin-1, GAP-43), modulating spine morphology and thus surface expression and synaptic localization of AMPA receptors, which temporarily suppresses LTP (15-23), all of which play a role in cognition, depression and neuropathic pain (18, 24-27).

Early clinical studies using TNF inhibitors (e.g. etanercept and infliximab) showed an inability to reduce mortality in sepsis patients (28, 29), which dampened enthusiasm for their use. More than 2 decades on, additional meta-analysis' of data in sepsis patients revealed an overall improvement in survival rates (30), when studies are sufficiently powered, which prompted a re-examination of their use. Subsequent studies modulating TNF activity under injury and ischemic conditions have shown some promising outcomes in both rodents and humans (31-35). Unfortunately, the TNF inhibitors have also shown an abundance of side-effects, warranting FDA blackbox warnings regarding possible immunological dysfunction and heart failure (36-38), and therefore the use of traditional TNF inhibitors should be cautioned in patients. These side-effects are likely due to the differences in TNF receptor subtype functions, that have complicated the TNF field until recently. TNF is a unique cytokine in that it is first produced as a transmembrane protein (tmTNF) that preferentially activates TNF receptor 2 (TNFR2: CD120b or p75/p80) (39), but once cleaved from the cell membrane TNF exists in a soluble form (solTNF) and preferentially activates TNF receptor 1 (TNFR1: CD120a or p55/p60) (39). Although both TNFR1 and TNFR2 can trigger some common signaling pathways (40), TNFR2 activation generally promotes beneficial outcomes such as cell survival,

induction of neurogenesis, and promotion of CNS autoimmunity (41-43), while TNFR1 activity generally promotes detrimental outcomes such as cell death, aberrant neuronal plasticity, and exacerbation of the existing inflammatory response (41, 44, 45). The fact that traditional TNF inhibitors (e.g. etanercept and infliximab) are unable to distinguish between the different TNF ligand or receptor subtypes, and thus inhibiting TNFR2 activity, is likely driving the development of unwanted side-effects.

For these reasons, a novel 'second generation' TNF inhibitor was developed that selectively impedes the activity of solTNF (XPro1595). XPro1595 has been successfully used in numerous pre-clinical inflammatory disease models (46-50), with no known side-effects. It can effectively cross the BBB (51), has a half-life of 19.1 hours (47), and can even improve heart function in a rodent model of cardiac arrest (52). In recent clinical trials, XPro1595 was shown to be safe and well tolerated in cancer patients (53), and interim data released from INmuneBio Inc. from a small clinical trial in Alzheimer's Disease patients shows the biologic (used at 1.0 mg/kg S.C.) reverses brain white matter inflammation and CSF inflammatory protein expression (54). Overlapping pathologies occur in brains following stroke, TBI and those with Alzheimer's Disease, therefore, we sought to investigate whether using XPro1595 to selectively bind and neutralize solTNF in a clinically relevant window following TBI in mice can improve pathophysiological and functional outcomes.

METHODS

Animals

Male C57Bl/6J mice aged 2 to 4 months were used for the current study. Animals were housed in a 12-hour light/dark cycle with food and water ad libitum. Procedures related to animal use were approved by the Virginia Commonwealth University Institutional Animal Care and Use Committee (in accordance with NIH care and use of laboratory animals).

Study Design

The study groups included TBI-injured and sham-injured mice, treated with XPro1595 (XP) or vehicle (V), that survived between 4 hours and 2 weeks. Animals surviving for 14 days underwent neurological testing, prior to having their brain collected for analysis.

Traumatic Brain Injury Model

Mice were anaesthetized with ketamine (75 mg/kg body weight) and xylazine (14 mg/kg body weight) by intraperitoneal injection and positioned in a stereotaxic frame. A 5-mm craniotomy was made using a portable drill over the right parietotemporal cortex (−2.5 mm caudal and 2.0 mm lateral from bregma). A drop of sterile saline was placed over the meninges to prevent it from drying out and tearing at the point of impact. A mild-to-moderate injury was generated (to avoid substantial structural damage to the underlying hippocampus) using a 3-mm beveled stainless-steel tip attached to an Impact One CCI device (Leica) at a velocity of 3.0 m/sec, depth of 0.5 mm, and 150 msec impact duration. Sham mice received anesthetic and skin incision only (since craniotomies themselves promote an inflammatory response). After CCI injury, the skin was sutured using 5-0 silk sutures. Starting 60 minutes post-injury, mice received twice weekly subcutaneous injections of XPro1595 (10 mg/kg in PBS, INmuneBio) or vehicle (0.1M PBS).

Histological Preparation, Staining and Immunohistochemistry

Mice were re-anaesthetized with ketamine (75 mg/kg) and xylazine (14 mg/kg) by intraperitoneal injection prior to transcardial perfusion or fresh brain dissection.

For qPCR analysis, fresh hippocampal tissue was dissected 6 hours post-injury (5 hours post-treatment), snap frozen in liquid nitrogen, and stored at -80oC. The frozen tissue was homogenized in RTL buffer (Qiagen) using lysing matrix D beads (MP Biomedicals). Total mRNA was extracted using RNeasy extraction kit (Qiagen) and converted to cDNA using reverse transcription kit (Applied Biosystems), followed by mRNA expression being processed using SYBRgreen real-time PCR (Applied Biosystems). Inflammatory cytokine expression for TNF, TNFR1, TNFR2, IL-6, and IL-1β was evaluated using Bio-

Rad mouse primers. Values were normalized to GAPDH expression, and expressed as a fold change within the ipsilateral tissue, as compared to the contralateral tissue.

For immunohistochemistry, transcardial perfusion was performed on WT and Thy1-YFPH mice, using approximately 15 ml of PBS, followed by approximately 25 ml of 4 % paraformaldehyde (Sigma). The brain was dissected, stored in 4 % paraformaldehyde for 2 hours, cryoprotected in 20 % sucrose in PBS for 48 hours, and then quickly frozen in OCT over isopentane on dry ice, and stored at -80 °C. Serial frozen coronal sections were cut 40 µm thick through the brain. Slides with sections from Thy1-YFPH mice containing hippocampus were washed in PBS to remove the OCT, and coverslipped in Prolong Gold Antifade mounting medium containing DAPI (Thermo Fisher). Slides with sections from WT mice containing hippocampus were permeabilized with 0.2 % triton X-100 (Sigma) in 2 % fish gel in PBS solution and immunohistochemically labelled with the primary antibody (1:2000 rabbit anti-GFAP, Dako; 1:2000 rabbit anti-IBA-1, Wako) overnight at 4 °C. Sections were washed 3 times in PBS, incubated in fluorescent secondary antibodies (1:500, Molecular Probes) for 30 min at room temperature, washed an additional 3 times in PBS, and coverslipped in the same mounting medium containing DAPI (ThermoFisher). Sections from WT and Thy1-YFP mice were photographed at 60x oil with equal exposure on a Zeiss AxioImager Z2 microscope, connected to a Zeiss Monochrome digital camera (AxioCam MRm) with Zeiss Zen Software (Blue Edition version 1.1.2.0).

For Western blotting, fresh frozen hippocampal tissue will be homogenized according to Dixon laboratory protocols in RIPA lysis buffer, reduced and denatured using Invitrogen SDS loading buffer, and run on Invitrogen pre-cast bis-tris gradient gels, prior to being transferred to nitrocellulose membranes. Proteins of interest will be detected using antibodies to TNF, TNFR1, TNFR2, IL-6, IL-1beta, and IL-10, prior to incubation with secondary antibody, and then chemiluminescence visualized using the Bio-Rad ChemiDoc machine, and quantitating band measurement using Bio-Rad One optical density calculation.

For Golgi labelling, transcardial perfusion was performed using approximately 15 ml of PBS, followed by approximately 25 ml of 4% paraformaldehyde. The brain was dissected and prepared according to FD Neurotechnology "Rapid Golgi stain" manufacturer's instructions. 100 µm thick sagittal cryostat sections were cut according to the manufacturer's instructions, and coverslipped in Permount mounting medium. Golgi-stained sections containing hippocampus were scanned for dendrites at least 200 µm in length in the CA1 region. These dendrites were photographed at 100x oil on a Zeiss AxioImager Z2 microscope using Köhler illumination, connected to a Q Imaging color digital camera (Model 2000R-F-CLR-12, 12-bit) with Neurolucida software (version 2020.2.4).

Histological Analysis

Glial reactivity within the ipsilateral and contralateral cortex and hippocampus was determined by quantitating GFAP and IBA-1 immunohistochemistry density, whereby images were converted to gray scale and thresholded in NIH ImageJ software (version 1.52a) to identify the area fraction of pixels positive for GFAP or IBA-1-immunoreactivity. Values for each photograph were averaged per section, per animal, and then per group. To assess dendritic degeneration, photographs of DCX-positive dendrites from immature neurons in the inner molecular layer of the dentate gyrus were quantitated for the presence (1) or absence (0) of dendritic beadings/swellings. Values for each photograph were averaged per section, per animal, and then per group. Subsequently, photographs of CA1 neurons from Thy1-YFP-H mice were inspected for the presence of dendritic beadings. To assess dendritic spine density, photographs of CA1 hippocampus containing Golgi-stained dendrites were quantitated to determine dendritic spine density. The number of dendritic spines along a dendritic segment 200 µm in length were counted, and expressed as the number of spines per 200 µm.

Neurological Testing

Morris Water Maze: Cognition (spatial learning and memory) was assessed on post-injury days 7 to 11. A blue plastic circular pool 5-foot wide and 11-inches deep was placed in the center of the room with large

(3-foot wide) visual cues placed on 3 of the 4 surrounding walls. The pool was divided into 4 quadrants, arbitrarily nominated North, South, East, and West, and a glass beaker 5-inches wide was covered in cotton gauze fabric and weighted upside down in the East quadrant of the pool. The mice were held by their tail and placed into the pool facing the pool edge, and were given 4 trials per day, starting from each of the 4 quadrants for 5 consecutive days. Quadrant order on each consecutive day was as follows: NWES, WNSE, EWSN, SEWN, NESW. The mice were allowed a maximum of 2 minutes to find the hidden platform, and if unsuccessful were gently lifted onto the platform and allowed to remain there for 20 seconds before being removed to their home cage. The number of quadrants the mice entered before reaching the platform, as well as time taken to reach the platform were measured. On post-injury day 14 (72 hours after the last trial) the mice underwent a probe trial, in which the platform from the East quadrant was removed from the pool, the mice placed in the opposite quadrant (West quadrant), and allowed a maximum of 30 seconds to 'find' the platform. Time spent in the East quadrant, and number of times entering the East quadrant were measured.

Sucrose Preference Test: Depressive-like behavior was assessed prior to injury, and on post-injury days 3, 7 and 14. Mice were housed individually for the duration of the test, and given free access to 2 water bottles filled with either regular water or 2% sucrose diluted in water (Acros Organics Sucrose) overnight (5pm to 9am). The amount of regular water versus sucrose water that each mouse drank was measured. Immediately after the test all mice were placed back into their group housing. Baseline testing was performed on 3 separate evenings, and any mouse that did not have a pre-injury preference for the sucrose solution was excluded from the analysis. The sucrose preference was calculated as the amount of sucrose drunk as a percentage of total liquid drunk.

Mechanical von Frey Test: Pre-clinical rodent models of TBI display periorbital and hindpaw neuropathic pain (55, 56). To assess the role of solTNF in the induction of injury-induced neuropathic pain, we measured the level of mechanical hypersensitivity underneath the animals ipsilateral hindpaw 3-, 7- and

14-days post-injury. In a dimly lit room, a 10" x 19" extension window screen (Thermwell) was fully extended and placed atop 2 polystyrene boxes, with a desk lamp placed behind and just under the height of the screen, angled towards the investigator. Four mice at a time were placed on top of the screen, with a 600 ml glass beaker (Pyrex) placed over the top of each mouse to prevent escape. A disposable underpad was draped over the beakers to minimize any light and/or movement stimulation. After 15 minutes acclimatization under the beaker, hindpaw hypersensitivity was assessed by holding the von Frey filament (Bioseb) handle under the screen, and slowly raising the end of the filament up through the screen to press against the under-side of the mouse's hindpaw walking pad until a slight bend was observed in the fiber. Continued advancement/bending of the filament does not necessarily produce more force of application. The investigator tested the lightest filament first, and sequentially tested up through the filament sizes until a positive result was established. A positive result was the mouse noticing 3 out of 5 consecutive tests for each filament, defined as the mouse withdrawing its foot, licking or shaking its foot, or rapidly moving its body away from the stimulus. Once a positive result was established for each mouse, the testing was concluded for that mouse for that day. The testing occurred as rapidly as possible to reduce restraint distress, although it was noticed that mice would often fall asleep during testing, which required gentle tapping from underneath the screen to wake up the animal.

Statistical Analysis

All data were assessed for homogeneity of variance, after which statistical analysis was performed. Histological differences were assessed using the Student's t-test, and behavioural differences (intra- and inter-group analysis) were assessed using two-way repeated measures analysis of variance with Student-Newman-Keuls method post hoc in SigmaPlot 13.0 where significance was <0.05. Data in figures are expressed as mean ± standard error of the mean.

RESULTS

Soluble TNF inhibition does not regulate IL-6 and IL-1β expression following TBI

We sought to determine whether selective inhibition of solTNF following TBI regulates mRNA expression of key inflammatory cytokines in select brain regions. We observed that neutralizing solTNF using XPro1595 did not change the expression of the key pro-inflammatory cytokines IL-6 and IL-1β in the peri-lesional cortex or ipsilateral hippocampus 6 hours following injury, compared to vehicle-treated injured mice (Figure 1A&B). Intriguingly, selective inhibition of solTNF significantly increased TNF expression in the hippocampus following TBI (Figure 1C), with a tendency for increased production in the peri-lesional region. We also examined TNFR1 expression, and observed a significant increase within the hippocampus (Figure 1D). No significant differences were observed in TNFR2 expression, although trends suggest slight increases in both hippocampus and peri-lesional region following injury (Figure 1E).

Soluble TNF inhibition reduces glial reactivity following TBI

To determine whether inhibiting solTNF attenuates injury-induced inflammation, mice were administered XPro1595 (10 mg/kg S.C.) or vehicle, starting 60 minutes following the TBI. After a 2-week survival period, we assessed glial reactivity by immunohistochemically labelling cortical and hippocampal tissue with antibodies against GFAP (astrocytes) and IBA-1 (microglial/macrophage). Only minimal GFAP and IBA-1 reactivity was detected in the uninjured hemisphere, independent of treatment (Figure 2A, B, G & H: contralateral hippocampus not shown). In comparison, GFAP is significantly upregulated in the cortical peri-lesional region hippocampal CA1 region, which is significantly attenuated by treatment with XPro1595 (Figure 2A-F, M&N). Injury also promoted an increase in IBA-1 expression in the cortical peri-lesional and hippocampal CA1 regions (Figure 2G-L, O&P), with XPro1595 treatment rescuing these effects back to baseline levels.

Soluble TNF inhibition prevents hippocampal dendritic degeneration following TBI

Thy-1 YFPH mice display endogenous fluorescent labelling of hippocampal neurons (Figure 3A), which in the CA1 regions of naïve mice exhibit long and wavy dendrites with an extensive number of post-synaptic spines (Figure 3A&B' and 3B' inset). Three days following TBI the dendrites appear disjointed, with

extensive dendritic swellings (beading), and an absence of spines (Figure 3B'' and 3B'' inset). Using immunohistochemistry to support the transgenic observations, we labeled hippocampal dendrites with doublecortin (immature dendrites), and also observed extensive dendritic swellings in the mouse hippocampal DG 14 days following TBI (Figure 3C); an affect that was significantly reduced in mice treated with XPro1595 (Figure 3C&D).

Soluble TNF inhibition prevents hippocampal dendritic plasticity following TBI

TBI was induced in mice and the expression of post-synaptic scaffolding protein PSD-95 was quantitated. We observed that PSD-95 expression was reduced 3 days following injury (Figure 4A), but which was prevented in injured mice treated with XPro1595. We next sought to determine whether our model of TBI reduced the density of hippocampal CA1 dendritic spines, and whether soluble TNF inhibition can rescue this effect. Mice were subjected to TBI and sacrificed 3 days later: a timepoint known to be consistent with reduced hippocampal dendritic spine density. The spine density of CA1 hippocampal neurons impregnated with Golgi stain was quantitated (Figure 5A). We observed that TBI reduced the density of dendritic spines in the CA1 hippocampal region (Figure 5B), but was unaffected in the injured mice treated with XPro1595 (Figure 5C).

Soluble TNF inhibition prevents TBI-induced functional deficits

Spatial Learning and Memory (Morris Water Maze): One of the most well-characterized neurological symptoms associated with hippocampal injury is cognitive impairment, specifically learning and memory (57). Therefore, we assessed the ability of mice to learn the MWM task for 5 consecutive days, on post-injury days 7 to 11. On the first day of testing the vehicle-treated injured mice were significantly less able to find the platform than sham-injured mice, although XPro1595-treated injured mice able to find the platform in the same amount of time as the sham-injured mice (Figure 5A). Notably, the vehicle-treated injured mice were also significantly less able to find the MWM platform than XPro1595-treated mice. In accordance with taking extra time to find the MWM platform, the vehicle-treated injured mice also

entered significantly more MWM quadrants to find the platform compare to XPro1595-treated injured mice (Figure 5B). Three days after the last MWM training day, the mice were tested in the MWM probe test (removal of platform). The vehicle-treated injured mice spent significantly less time in the platform quadrant compared to sham-injured mice (Figure 5C), and showed a strong tendency to spend less time in the platform quadrant compared to XPro1595-treated injured mice. Similarly, the XPro1595-treated injured mice also entered the platform quadrant more times than the vehicle-treated injured mice (Figure 5D).

Depressive-like Behavior (Sucrose Preference Test): In addition to cognitive impairment, depression is frequently associated with aberrant hippocampal pathology following TBI. Therefore, we assessed the development of depressive-like symptoms in brain-injured mice, using the sucrose preference test prior to injury and on post-injury days 3, 7 and 14. Prior to injury the naïve uninjured untreated mice showed approximately 90% preference for the sucrose solution (Figure 5E), but this was significantly reduced in vehicle-treated mice acutely following injury, suggesting the CCI brain injury model promotes depressive-like symptoms. Conversely, treating injured mice systemically with XPro1595 prevented a reduction in their preference for the 2% sucrose solution, suggesting that XPro1595 affects the onset of depressive-like symptoms and may be a useful clinical tool.

Hindpaw Neuropathic Pain (Mechanical von Frey Assay): Since depression and pain are frequently comorbid following TBI, individuals with injury-induced chronic pain are at risk of developing dermal mechanical and thermal hypersensitivity (58), we used the mechanical von Frey assay to assess hindpaw hypersensitivity. Mice underwent testing prior to injury and on post-injury days 3, 7 and 14. We observed that all sham injured animals, independent of treatment, experienced a small increase in hypersensitivity 3 days following injury (indicated by reduced mechanical threshold: Figure 5F), but this was transient and quickly returned to baseline levels. In comparison, vehicle-treated injured mice were significantly more hypersensitive on day 3 (almost a 3-fold increase compared to vehicle-treated sham

mice), and this remained until the end of testing on day 14, suggesting these mice were in more pain, which lasted longer than sham-operated mice. Conversely, XPro1595-treated injured mice experienced less hypersensitivity than vehicle-treated injured mice (1.6-fold increase compared to XPro1595-treated sham mice), and this quickly improved so that mice were no longer experiencing significantly greater hypersensitivity at the end of testing. This suggests that XPro1595 therapy can reduce levels of pain associated with brain injury.

DISCUSSION

Mild TBI is often associated with cognitive impairment, with many individuals experiencing significant improvement over the first few months following an injury, although a non-trivial number may develop persistent impairments. Importantly, cognitive impairment is strongly associated with the development of depression, along with chronic pain, anxiety, and stress (18, 59-63). In individuals experiencing chronic pain, symptoms often manifests as musculoskeletal pain (neck, shoulders, and back) and/or post-traumatic headaches (64), many of whom also experience comorbid neuropathic pain (termed 'central pain') (58, 65).

The hippocampus plays an important role in regulating learning and memory, and structurally is composed of a tri-synaptic neural circuit (66-68). This tri-synaptic circuit is composed of the performant pathway projecting from the entorhinal cortex to the hippocampal DG, after which mossy fibers project from the DG to synapse on pyramidal cells within the CA3 region, and then Schaffer collaterals project from the CA3 region to the CA1. Within this circuit, axon terminals synapse onto dendritic spines, releasing glutamate from pre-synaptic terminals to activate AMPA receptors located within spines on the post-synaptic dendrite to generate a miniature excitatory postsynaptic current (mEPSCs) that modulates efferent connectivity (i.e. long-term potentiation, LTP) (15, 69). An individual's loss of memory is commonly known to be due to damage anywhere along the hippocampal tri-synaptic neuronal circuit (70-72), but the hippocampus also plays a role in the formation and retrieval of negative emotional memory, that is associated with pain and depression (18, 20, 27, 73). Importantly, all of these symptoms share overlapping neuronal plasticity

pathology, including reduced pre-synaptic puncta density, synaptic protein expression (PSD-95, synapsin-1, GAP-43), and post-synaptic dendritic spine density (particularly mushroom spines), that collectively inhibit LTP (excitatory synaptic connectivity) (17, 18, 60, 72, 74-79), but which also includes dendritic degeneration in the form of dendritic "beads" or "swellings" (72, 76), likely due to blockade of protein and mitochondrial trafficking. While TBI causes a sustained upregulation of cytokines, such as interleukin 1-beta (IL-1β), IL-6 and TNF (12-14), TNF is unique in that its function is dependent upon activation of receptor subtype (TNFR1 and TNFR2), and a strong connection exists between TNF/TNFR1-mediated hippocampal plasticity, and impaired neurological outcomes (18, 25, 27). Under physiologic conditions, TNF regulates AMPA receptor surface expression (homeostatic synaptic plasticity), which subsequently regulates mEPSC currents and eventually LTP (80, 81), although excess production of solTNF under pathological conditions activates TNFR1 to promote reductions in dendritic spine density, length, and protein expression (PSD-95, synapsin-1, GAP-43), modulating spine morphology and surface expression and synaptic localization of AMPA receptors, which temporarily suppresses LTP to modulate cortical connectivity (15-23). Additionally, the induction of beading and degeneration causing impaired protein and mitochondrial transport along dendrites (72, 76, 82, 83), is also known to be induced by TNF (82). Therefore, selectively inhibiting solTNF/TNFR1 activity is critically important following TBI.

Following injury, TNF and TNFR1 expression increases, peaking between 4 and 24 hours post-injury (13, 45) (dependent on the animal model used (84)). Therefore, acute administration of XPro1595 (1 hour post-injury) in the current studies is not only clinically relevant, but is preventing activation of TNFR1 prior to the injury-induced peak of TNF/TNFR1 expression. Our observation that XPro1595 treatment does not change the expression pattern of the other key inflammatory cytokines within the hippocampus or peri-lesional region is important given that both IL1-β and IL-6 are both pro- and anti-inflammatory following trauma (14, 85). Reducing their expression may prevent their contribution to brain repair mechanisms, while increasing their expression may exacerbate the extent of the injury. Interestingly, increases in TNF and TNFR1 expression were observed in the XPro1595-treated injured mice, similar to antagonist induced

receptor upregulation (86, 87), although this is functionally inconsequential given that the biologic neutralizes any available solTNF present. Indeed, the increased TNF expression observed is likely beneficial allowing for increased tmTNF/TNFR2 activity within the injury milieu. Importantly however, XPro1595 treatment significantly reduced astrogliosis in all areas measured, as well as significantly reducing cortical microglial reactivity (with a trend to reduce hippocampal microglial reactivity), when measured two weeks post- injury. Therefore, it is plausible to suggest that despite TNF and TNFR1 upregulation, XPro1595 treatment reduced TNFR1 activity levels, although future studies investigating TNFR1 downstream activities are needed to confirm this.

Intriguingly, we did not observe a significant upregulation of hippocampal microglial activation in this mild-to-moderate TBI model. Previous studies using the same injury model, but with a larger injury severity (5m/s velocity) show robust microglial reactivity (88), suggesting that this milder injury (3m/s velocity) may not cause the same extent of hippocampal inflammation, since microglia are thought to be the main de novo producers of TNF (despite astrocytes and neurons also expressing TNF post-injury). None-the-less, injury-induced alterations in hippocampal pathology were observed, suggesting that even small levels of glial reactivity can promote detrimental changes to neuronal plasticity, including pathology known to regulate cognitive impairment, depression and pain.

Although hippocampal synaptic plasticity (spine density) is known to occur in a bi-phasic manner with the greatest spine loss occurring within 2-3 days post-injury (72, 76) (our own data supports this notion), the time-course of dendritic degeneration is less well characterized. Our data adds to the literature that initial dendritic degeneration occurs within 3 days post-injury, and persists through to 14 days post-injury, even being observed in newly developing immature dendrites (DCX-positive), thus the effects of even a mild-to-moderate injury are long-lasting. Although some dendritic degeneration was observed in injured mice treated with XPro1595, the amount of degeneration was significantly less, lending support for the beneficial effects of XPro1595 administered acutely following TBI.

Our study also assessed functional outcomes known to be associated with the hippocampus. The data shows that injury-induced impairments in spatial learning (cognitive testing), as well as sucrose preference (depressive-like behavior) and dermal hypersensitivity (neuropathic pain), the latter being clinically relevant to the large number of individuals experiencing post-traumatic headaches. Since XPro1595 was administered in a clinically relevant manner (subcutaneously), the ability of altered pathology in other brain structures that may be contributing to the observed functional improvements following treatment cannot be ruled out. None-the-less, the improvements in TBI pathology and associated functional outcomes, combined with a lack of known side-effects in both animal models and patients, supports the use of XPro1595 clinically in patients with TBI.

CONCLUSION

Excess levels of the inflammatory cytokine TNF play a prominent role in many inflammatory disease pathologies, including the induction of aberrant pathology following a traumatic brain injury. Attempts to use TNF receptor fusion proteins or monoclonal antibodies to regulate this cytokines function have shown some successes clinically, but has been fraught with complications due to their numerous adverse side-effects. Our data provide support for the clinical use of a novel "second generation" TNF inhibitor XPro1595 that selectively inhibits only the detrimental soluble form of TNF to prevent the disease sequelae, while sparing the beneficial transmembrane form of TNF to allow reparative cellular mechanisms to remain.

ABBREVIATIONS

LTP	long term potentiation
solTNF	soluble form of tumor necrosis factor
tmTNF	transmembrane form of tumor necrosis factor
TNFR1	tumor necrosis factor receptor 1
TNFR2	tumor necrosis factor receptor 2

DECLARATIONS

Ethics Approval and Consent to Participate

All experiments were performed under approval of the VCU Institutional Animal Care and Use Committee.

Consent for Publication

Not applicable.

Availability of Data and Materials

The authors are always willing to collaborate and datasets generated and/or analyzed during the current study are available from the corresponding author on reasonable request.

Competing Interests

The authors declare that they have no competing interests.

Funding

These studies were funded by a grant from the Virginia Commonwealth Neurotrauma Initiative (to KJD (FP00001476)), and a donation of $5,000 from Dr. Randall Merchant using MCVF funds (to KJD). Microscopy was performed at the VCU Massey Cancer Center Microscopy Core Facility and supported, in part, with funding from NIH-NCI Cancer Center Support Grant P30 CA016059. Funding bodies did not contribute to the design of study or collection, analysis, interpretation of data or writing of the manuscript.

Author's Contributions

KL, MD, RR and NNL performed the experiments and tabulated the data. KJD designed, planned, funded, analyzed and interpreted the data. All authors read and approved the final manuscript.

Acknowledgements

We thank Dr. Eleonora Mezzaroma for assisting with the qPCR protocol, and INmuneBio Inc. for providing XPro1595 free of charge.

REFERENCES

1. Shively S, Scher AI, Perl DP, Diaz-Arrastia R. Dementia resulting from traumatic brain injury: what is the pathology? Arch Neurol. 2012;69(10):1245-51.
2. Luo C, Jiang J, Lu Y, Zhu C. Spatial and temporal profile of apoptosis following lateral fluid percussion brain injury. Chin J Traumatol. 2002;5(1):24-7.
3. Raghupathi R. Cell death mechanisms following traumatic brain injury. Brain Pathol. 2004;14(2):215-22.
4. O'Connor CA, Cernak I, Vink R. The temporal profile of edema formation differs between male and female rats following diffuse traumatic brain injury. Acta Neurochir Suppl. 2006;96:121-4.
5. Lotocki G, de Rivero Vaccari JP, Perez ER, Sanchez-Molano J, Furones-Alonso O, Bramlett HM, et al. Alterations in blood-brain barrier permeability to large and small molecules and leukocyte accumulation after traumatic brain injury: effects of post-traumatic hypothermia. J Neurotrauma. 2009;26(7):1123-34.
6. Morganti-Kossman MC, Lenzlinger PM, Hans V, Stahel P, Csuka E, Ammann E, et al. Production of cytokines following brain injury: beneficial and deleterious for the damaged tissue. Mol Psychiatry. 1997;2(2):133-6.
7. Ghirnikar RS, Lee YL, Eng LF. Inflammation in traumatic brain injury: role of cytokines and chemokines. Neurochem Res. 1998;23(3):329-40.
8. Lossinsky AS, Shivers RR. Structural pathways for macromolecular and cellular transport across the blood-brain barrier during inflammatory conditions. Review. Histol Histopathol. 2004;19(2):535-64.
9. Taupin P. Adult neurogenesis, neuroinflammation and therapeutic potential of adult neural stem cells. Int J Med Sci. 2008;5(3):127-32.
10. Ekmark-Lewen S, Lewen A, Israelsson C, Li GL, Farooque M, Olsson Y, et al. Vimentin and GFAP responses in astrocytes after contusion trauma to the murine brain. Restor Neurol Neurosci. 2010;28(3):311-21.
11. Homsi S, Piaggio T, Croci N, Noble F, Plotkine M, Marchand-Leroux C, et al. Blockade of acute microglial activation by minocycline promotes neuroprotection and reduces locomotor hyperactivity after closed head injury in mice: a twelve-week follow-up study. J Neurotrauma. 2010;27(5):911-21.
12. Yang SH, Gangidine M, Pritts TA, Goodman MD, Lentsch AB. Interleukin 6 mediates neuroinflammation and motor coordination deficits after mild traumatic brain injury and brief hypoxia in mice. Shock. 2013;40(6):471-5.
13. Lotocki G, Alonso OF, Dietrich WD, Keane RW. Tumor necrosis factor receptor 1 and its signaling intermediates are recruited to lipid rafts in the traumatized brain. J Neurosci. 2004;24(49):11010-6.
14. Murray KN, Parry-Jones AR, Allan SM. Interleukin-1 and acute brain injury. Front Cell Neurosci. 2015;9:18.
15. He P, Liu Q, Wu J, Shen Y. Genetic deletion of TNF receptor suppresses excitatory synaptic transmission via reducing AMPA receptor synaptic localization in cortical neurons. FASEB J. 2012;26(1):334-45.
16. Albensi BC, Mattson MP. Evidence for the involvement of TNF and NF-kappaB in hippocampal synaptic plasticity. Synapse. 2000;35(2):151-9.
17. Liu Y, Zhou LJ, Wang J, Li D, Ren WJ, Peng J, et al. TNF-alpha Differentially Regulates Synaptic Plasticity in the Hippocampus and Spinal Cord by Microglia-Dependent Mechanisms after Peripheral Nerve Injury. J Neurosci. 2017;37(4):871-81.
18. Dellarole A, Morton P, Brambilla R, Walters W, Summers S, Bernardes D, et al. Neuropathic pain-induced depressive-like behavior and hippocampal neurogenesis and plasticity are dependent on TNFR1 signaling. Brain Behav Immun. 2014;41:65-81.
19. Mutso AA, Petre B, Huang L, Baliki MN, Torbey S, Herrmann KM, et al. Reorganization of hippocampal functional connectivity with transition to chronic back pain. J Neurophysiol. 2014;111(5):1065-76.

20. Cardoso-Cruz H, Lima D, Galhardo V. Impaired spatial memory performance in a rat model of neuropathic pain is associated with reduced hippocampus-prefrontal cortex connectivity. J Neurosci. 2013;33(6):2465-80.
21. Chang Y, Yan LH, Zhang FK, Gong KR, Liu MG, Xiao Y, et al. Spatiotemporal characteristics of pain-associated neuronal activities in primary somatosensory cortex induced by peripheral persistent nociception. Neurosci Lett. 2008;448(1):134-8.
22. Nakamura H, Katayama Y, Kawakami Y. Hippocampal CA1/subiculum-prefrontal cortical pathways induce plastic changes of nociceptive responses in cingulate and prelimbic areas. BMC Neurosci. 2010;11:100.
23. Becker D, Deller T, Vlachos A. Tumor necrosis factor (TNF)-receptor 1 and 2 mediate homeostatic synaptic plasticity of denervated mouse dentate granule cells. Sci Rep. 2015;5:12726.
24. Hennessy E, Gormley S, Lopez-Rodriguez AB, Murray C, Murray C, Cunningham C. Systemic TNF-alpha produces acute cognitive dysfunction and exaggerated sickness behavior when superimposed upon progressive neurodegeneration. Brain Behav Immun. 2017;59:233-44.
25. Postal M, Lapa AT, Sinicato NA, de Oliveira Pelicari K, Peres FA, Costallat LT, et al. Depressive symptoms are associated with tumor necrosis factor alpha in systemic lupus erythematosus. J Neuroinflammation. 2016;13:5.
26. Gerard E, Spengler RN, Bonoiu AC, Mahajan SD, Davidson BA, Ding H, et al. Chronic constriction injury-induced nociception is relieved by nanomedicine-mediated decrease of rat hippocampal tumor necrosis factor. Pain. 2015;156(7):1320-33.
27. Martuscello RT, Spengler RN, Bonoiu AC, Davidson BA, Helinski J, Ding H, et al. Increasing TNF levels solely in the rat hippocampus produces persistent pain-like symptoms. Pain. 2012;153(9):1871-82.
28. Grau GE, Maennel DN. TNF inhibition and sepsis -- sounding a cautionary note. Nat Med. 1997;3(11):1193-5.
29. Fisher CJ, Jr., Agosti JM, Opal SM, Lowry SF, Balk RA, Sadoff JC, et al. Treatment of septic shock with the tumor necrosis factor receptor:Fc fusion protein. The Soluble TNF Receptor Sepsis Study Group. N Engl J Med. 1996;334(26):1697-702.
30. Qiu P, Cui X, Sun J, Welsh J, Natanson C, Eichacker PQ. Antitumor necrosis factor therapy is associated with improved survival in clinical sepsis trials: a meta-analysis. Crit Care Med. 2013;41(10):2419-29.
31. Tobinick E, Kim NM, Reyzin G, Rodriguez-Romanacce H, DePuy V. Selective TNF inhibition for chronic stroke and traumatic brain injury: an observational study involving 629 consecutive patients treated with perispinal etanercept. CNS Drugs. 2012;26(12):1051-70.
32. Tobinick E, Rodriguez-Romanacce H, Levine A, Ignatowski TA, Spengler RN. Immediate neurological recovery following perispinal etanercept years after brain injury. Clin Drug Investig. 2014;34(5):361-6.
33. Baratz R, Tweedie D, Rubovitch V, Luo W, Yoon JS, Hoffer BJ, et al. Tumor necrosis factor-alpha synthesis inhibitor, 3,6'-dithiothalidomide, reverses behavioral impairments induced by minimal traumatic brain injury in mice. J Neurochem. 2011;118(6):1032-42.
34. Chio CC, Chang CH, Wang CC, Cheong CU, Chao CM, Cheng BC, et al. Etanercept attenuates traumatic brain injury in rats by reducing early microglial expression of tumor necrosis factor-alpha. BMC Neurosci. 2013;14:33.
35. Chio CC, Lin JW, Chang MW, Wang CC, Kuo JR, Yang CZ, et al. Therapeutic evaluation of etanercept in a model of traumatic brain injury. J Neurochem. 2010;115(4):921-9.
36. Kwon HJ, Cote TR, Cuffe MS, Kramer JM, Braun MM. Case reports of heart failure after therapy with a tumor necrosis factor antagonist. Ann Intern Med. 2003;138(10):807-11.

37. Thomas SS, Borazan N, Barroso N, Duan L, Taroumian S, Kretzmann B, et al. Comparative Immunogenicity of TNF Inhibitors: Impact on Clinical Efficacy and Tolerability in the Management of Autoimmune Diseases. A Systematic Review and Meta-Analysis. BioDrugs. 2015;29(4):241-58.
38. Maneiro JR, Salgado E, Gomez-Reino JJ. Immunogenicity of monoclonal antibodies against tumor necrosis factor used in chronic immune-mediated Inflammatory conditions: systematic review and meta-analysis. JAMA Intern Med. 2013;173(15):1416-28.
39. Fischer R, Marsal J, Gutta C, Eisler SA, Peters N, Bethea JR, et al. Novel strategies to mimic transmembrane tumor necrosis factor-dependent activation of tumor necrosis factor receptor 2. Sci Rep. 2017;7(1):6607.
40. Wajant H, Siegmund D. TNFR1 and TNFR2 in the Control of the Life and Death Balance of Macrophages. Front Cell Dev Biol. 2019;7:91.
41. Longhi L, Perego C, Ortolano F, Aresi S, Fumagalli S, Zanier ER, et al. Tumor necrosis factor in traumatic brain injury: effects of genetic deletion of p55 or p75 receptor. J Cereb Blood Flow Metab. 2013;33(8):1182-9.
42. Faustman DL, Davis M. TNF Receptor 2 and Disease: Autoimmunity and Regenerative Medicine. Front Immunol. 2013;4:478.
43. Atretkhany KN, Mufazalov IA, Dunst J, Kuchmiy A, Gogoleva VS, Andruszewski D, et al. Intrinsic TNFR2 signaling in T regulatory cells provides protection in CNS autoimmunity. Proc Natl Acad Sci U S A. 2018;115(51):13051-6.
44. Yang J, You Z, Kim HH, Hwang SK, Khuman J, Guo S, et al. Genetic analysis of the role of tumor necrosis factor receptors in functional outcome after traumatic brain injury in mice. J Neurotrauma. 2010;27(6):1037-46.
45. Knoblach SM, Fan L, Faden AI. Early neuronal expression of tumor necrosis factor-alpha after experimental brain injury contributes to neurological impairment. J Neuroimmunol. 1999;95(1-2):115-25.
46. Brambilla R, Ashbaugh JJ, Magliozzi R, Dellarole A, Karmally S, Szymkowski DE, et al. Inhibition of soluble tumour necrosis factor is therapeutic in experimental autoimmune encephalomyelitis and promotes axon preservation and remyelination. Brain. 2011;134(Pt 9):2736-54.
47. Clausen BH, Degn M, Martin NA, Couch Y, Karimi L, Ormhoj M, et al. Systemically administered anti-TNF therapy ameliorates functional outcomes after focal cerebral ischemia. J Neuroinflammation. 2014;11:203.
48. MacPherson KP, Sompol P, Kannarkat GT, Chang J, Sniffen L, Wildner ME, et al. Peripheral administration of the soluble TNF inhibitor XPro1595 modifies brain immune cell profiles, decreases beta-amyloid plaque load, and rescues impaired long-term potentiation in 5xFAD mice. Neurobiol Dis. 2017;102:81-95.
49. Cavanagh C, Tse YC, Nguyen HB, Krantic S, Breitner JC, Quirion R, et al. Inhibiting tumor necrosis factor-alpha before amyloidosis prevents synaptic deficits in an Alzheimer's disease model. Neurobiol Aging. 2016;47:41-9.
50. Sama DM, Mohmmad Abdul H, Furman JL, Artiushin IA, Szymkowski DE, Scheff SW, et al. Inhibition of soluble tumor necrosis factor ameliorates synaptic alterations and Ca2+ dysregulation in aged rats. PLoS One. 2012;7(5):e38170.
51. Karamita M, Barnum C, Mobius W, Tansey MG, Szymkowski DE, Lassmann H, et al. Therapeutic inhibition of soluble brain TNF promotes remyelination by increasing myelin phagocytosis by microglia. JCI Insight. 2017;2(8).
52. Wang C, Yang J, Z. H, Guo Q, Wu X, Bradley J, et al., editors. XPro1595 reduces the severity of post resuscitation myocardial dysfunction in a rat model of cardiac arrest. Circulation; 2018.
53. INmuneBioInc. INmune Bio Announces Final Phase I Clinical Data for its Soluble TNF Inhibitor, INB03, Demonstrates Efficacy and Safety; INB03 is Advancing to Phase II Trials. https://wwwglobenewswirecom/news-release/2019/12/17/1961610/0/en/INmune-Bio-Announces-

570 Final-Phase-I-Clinical-Data-for-its-Soluble-TNF-Inhibitor-INB03-Demonstrates-Efficacy-and-Safety-INB03-
571 is-Advancing-to-Phase-II-Trialshtml. 2019.
572 54. INmuneBioInc. INmune Bio, Inc. Announces XPro1595 Found to Decrease Neuroinflammation and
573 Neurodegeneration Biomarkers in Patients with Alzheimer's Disease in Phase 1b Trial
574 https://www.globenewswire.com/news-release/2021/01/21/2162007/0/en/INmune-Bio-Inc-
575 Announces-XPro1595-Found-to-Decrease-Neuroinflammation-and-Neurodegeneration-Biomarkers-in-
576 Patients-with-Alzheimer-s-Disease-in-Phase-1b-Trial.html2021 [
577 55. Elliott MB, Oshinsky ML, Amenta PS, Awe OO, Jallo JI. Nociceptive neuropeptide increases and
578 periorbital allodynia in a model of traumatic brain injury. Headache. 2012;52(6):966-84.
579 56. Macolino CM, Daiutolo BV, Albertson BK, Elliott MB. Mechanical alloydnia induced by traumatic
580 brain injury is independent of restraint stress. J Neurosci Methods. 2014;226:139-46.
581 57. Akhondzadeh S. Hippocampal synaptic plasticity and cognition. J Clin Pharm Ther. 1999;24(4):241-
582 8.
583 58. Ofek H, Defrin R. The characteristics of chronic central pain after traumatic brain injury. Pain.
584 2007;131(3):330-40.
585 59. Sullivan-Singh SJ, Sawyer K, Ehde DM, Bell KR, Temkin N, Dikmen S, et al. Comorbidity of pain and
586 depression among persons with traumatic brain injury. Arch Phys Med Rehabil. 2014;95(6):1100-5.
587 60. Qiao H, Li MX, Xu C, Chen HB, An SC, Ma XM. Dendritic Spines in Depression: What We Learned
588 from Animal Models. Neural Plast. 2016;2016:8056370.
589 61. Bay E, Kirsch N, Gillespie B. Chronic stress conditions do explain posttraumatic brain injury
590 depression. Res Theory Nurs Pract. 2004;18(2-3):213-28.
591 62. Karson A, Demirtas T, Bayramgurler D, Balci F, Utkan T. Chronic administration of infliximab (TNF-
592 alpha inhibitor) decreases depression and anxiety-like behaviour in rat model of chronic mild stress. Basic
593 Clin Pharmacol Toxicol. 2013;112(5):335-40.
594 63. Grandhi R, Tavakoli S, Ortega C, Simmonds MJ. A Review of Chronic Pain and Cognitive, Mood,
595 and Motor Dysfunction Following Mild Traumatic Brain Injury: Complex, Comorbid, and/or Overlapping
596 Conditions? Brain Sci. 2017;7(12).
597 64. Nampiaparampil DE. Prevalence of chronic pain after traumatic brain injury: a systematic review.
598 JAMA. 2008;300(6):711-9.
599 65. Defrin R, Gruener H, Schreiber S, Pick CG. Quantitative somatosensory testing of subjects with
600 chronic post-traumatic headache: implications on its mechanisms. Eur J Pain. 2010;14(9):924-31.
601 66. Kumar RG, Gao S, Juengst SB, Wagner AK, Fabio A. The effects of post-traumatic depression on
602 cognition, pain, fatigue, and headache after moderate-to-severe traumatic brain injury: a thematic review.
603 Brain Inj. 2018;32(4):383-94.
604 67. Phillips KF, Deshpande LS. Repeated low-dose organophosphate DFP exposure leads to the
605 development of depression and cognitive impairment in a rat model of Gulf War Illness. Neurotoxicology.
606 2016;52:127-33.
607 68. Grzegorski T, Losy J. Cognitive impairment in multiple sclerosis - a review of current knowledge
608 and recent research. Rev Neurosci. 2017;28(8):845-60.
609 69. Kusters R, Kapitein LC, Hoogenraad CC, Storm C. Shape-induced asymmetric diffusion in dendritic
610 spines allows efficient synaptic AMPA receptor trapping. Biophys J. 2013;105(12):2743-50.
611 70. Mahmmoud RR, Sase S, Aher YD, Sase A, Groger M, Mokhtar M, et al. Spatial and Working
612 Memory Is Linked to Spine Density and Mushroom Spines. PLoS One. 2015;10(10):e0139739.
613 71. Leuner B, Gould E. Structural plasticity and hippocampal function. Annu Rev Psychol.
614 2010;61:111-40, C1-3.
615 72. Gao X, Deng P, Xu ZC, Chen J. Moderate traumatic brain injury causes acute dendritic and synaptic
616 degeneration in the hippocampal dentate gyrus. PLoS One. 2011;6(9):e24566.

73. Fasick V, Spengler RN, Samankan S, Nader ND, Ignatowski TA. The hippocampus and TNF: Common links between chronic pain and depression. Neurosci Biobehav Rev. 2015;53:139-59.
74. Yan BC, Park JH, Ahn JH, Lee JC, Won MH, Kang IJ. Postsynaptic density protein (PSD)-95 expression is markedly decreased in the hippocampal CA1 region after experimental ischemia-reperfusion injury. J Neurol Sci. 2013;330(1-2):111-6.
75. Wakade C, Sukumari-Ramesh S, Laird MD, Dhandapani KM, Vender JR. Delayed reduction in hippocampal postsynaptic density protein-95 expression temporally correlates with cognitive dysfunction following controlled cortical impact in mice. J Neurosurg. 2010;113(6):1195-201.
76. Scheff SW, Price DA, Hicks RR, Baldwin SA, Robinson S, Brackney C. Synaptogenesis in the hippocampal CA1 field following traumatic brain injury. J Neurotrauma. 2005;22(7):719-32.
77. Ansari MA, Roberts KN, Scheff SW. Oxidative stress and modification of synaptic proteins in hippocampus after traumatic brain injury. Free Radic Biol Med. 2008;45(4):443-52.
78. Ren WJ, Liu Y, Zhou LJ, Li W, Zhong Y, Pang RP, et al. Peripheral nerve injury leads to working memory deficits and dysfunction of the hippocampus by upregulation of TNF-alpha in rodents. Neuropsychopharmacology. 2011;36(5):979-92.
79. Winston CN, Chellappa D, Wilkins T, Barton DJ, Washington PM, Loane DJ, et al. Controlled cortical impact results in an extensive loss of dendritic spines that is not mediated by injury-induced amyloid-beta accumulation. J Neurotrauma. 2013;30(23):1966-72.
80. Stellwagen D, Malenka RC. Synaptic scaling mediated by glial TNF-alpha. Nature. 2006;440(7087):1054-9.
81. Becker D, Zahn N, Deller T, Vlachos A. Tumor necrosis factor alpha maintains denervation-induced homeostatic synaptic plasticity of mouse dentate granule cells. Front Cell Neurosci. 2013;7:257.
82. Kim JY, Shen S, Dietz K, He Y, Howell O, Reynolds R, et al. HDAC1 nuclear export induced by pathological conditions is essential for the onset of axonal damage. Nat Neurosci. 2010;13(2):180-9.
83. Greenwood SM, Mizielinska SM, Frenguelli BG, Harvey J, Connolly CN. Mitochondrial dysfunction and dendritic beading during neuronal toxicity. J Biol Chem. 2007;282(36):26235-44.
84. Woodcock T, Morganti-Kossmann MC. The role of markers of inflammation in traumatic brain injury. Front Neurol. 2013;4:18.
85. Scheller J, Chalaris A, Schmidt-Arras D, Rose-John S. The pro- and anti-inflammatory properties of the cytokine interleukin-6. Biochim Biophys Acta. 2011;1813(5):878-88.
86. Yoburn BC, Billings B, Duttaroy A. Opioid receptor regulation in mice. J Pharmacol Exp Ther. 1993;265(1):314-20.
87. Wonnacott S. The paradox of nicotinic acetylcholine receptor upregulation by nicotine. Trends Pharmacol Sci. 1990;11(6):216-9.
88. Dixon KJ, Theus MH, Nelersa CM, Mier J, Travieso LG, Yu TS, et al. Endogenous neural stem/progenitor cells stabilize the cortical microenvironment after traumatic brain injury. J Neurotrauma. 2015;32(11):753-64.

FIGURE LEGENDS

Figure 1: Pro-inflammatory cytokine expression 6 hours following TBI. Graphs show the fold change of expression within the ipsilateral tissue, as compared to the contralateral tissue of IL-6 **(A)**, IL-1β **(B)**, TNF **(C)**, TNFR1 **(D)**, and TNFR2 **(E)**, with either vehicle or XPro1595 treatment. qPCR analysis reveals selective inhibition of soluble TNF does not alter IL-6 or IL-1 β expression. In contract, XPro1595

significantly increased TNF and TNFR1 expression within the hippocampus, with a tendency for increased expression of TNFR2. Hipp=Hippocampal; V=Vehicle; XP=XPro1595; TBI+Veh = white bars; TBI+XP = grey bars; n=4 per group; * $p<0.05$.

Figure 2: Glial reactivity in the peri-lesional cortex and hippocampus two weeks following TBI. Negligible GFAP (astrocytes) and IBA-1 (microglia/macrophages) protein is expressed in the uninjured cortex **(A,B,G&H)**, and hippocampus (images not shown), independent of treatment. TBI promotes gliosis in both the peri-lesional region and hippocampus **(C,E,I&K)**, although this is prevented by using XPro1595 to neutralize soluble TNF **(D, F, J & L)**. Graphs show semi-quantitation of glial reactivity in the ipsilateral and contralateral hemisphere following TBI **(M-P)**. C-V = contralateral hemisphere+vehicle; C-XP = contralateral hemisphere+XPro1595; I-V = ipsilateral hemisphere+vehicle; I-XP = ipsilateral hemisphere+ XPro1595; TBI+V n=9, TBI+XP n=9; ** = $p<0.01$, *** = $p<0.001$. Scalebar in L = 50 µm.

Figure 3: Hippocampal dendritic degeneration following CCI injury. Thy1-YFP-labelled mouse hippocampus showing dentate gyrus (DG), CA1, CA2 and CA3 regions **(A)**. Neuronal dendrites from CA1 region in naive mice show normal morphology **(B')**, while 3 days post-injury CA1 dendrites develop abnormalities **(B'')**. CCI-injury appears to reduce spine density, and promotes swellings (beading) along the length of the dendrite **(B)**. In naïve uninjured animals, dendrites from immature neurons within the hippocampal DG that are immunoreactive for doublecortin, show an absence of dendritic swellings **(C')**. However, extensive swellings are observed on immature dendrites of the DG 14 days following the injury **(C'')** that can be significantly reduced when XPro1595 is administered starting 60 minutes post-injury **(C'''&D)**. V=Vehicle; XP=XPro1595; TBI+V n=4, TBI+XP n=4; * = $p<0.05$; Scalebar in B = 20 µm, B inset = 5 µm, and C = 2 µm.

Figure 4: TBI regulates hippocampal dendritic plasticity via soluble TNF activity. The ipsilateral hippocampus was semi-quantitated for PSD-95 expression; a prominent post-synaptic scaffolding protein,

686 3 days post-CCI injury. Western blot analysis reveals injury reduced hippocampal PSD-95 expression **(A)**,
687 which was prevented in mice treated with XPro1595 one-hour post-injury. **(B)** Morphology of Golgi-
688 stained hippocampal slices from sham- and CCI-injured mice, treated with either XPro1595 or Vehicle
689 show changes in spine density. Golgi-stained dendrites were quantitated for spine density (number of
690 spines on a dendrite 200 µm in length), revealing that injury reduces dendritic spine density **(C)**, which is
691 prevented in the XPro1595-treated injured mice. Veh=Vehicle, XP=XPro1595; (A) n=3 per group, (C)
692 Sham+Veh n=7, Sham+XP n=5, TBI+Veh n=10, TBI+XP n=10; ** = $p<0.01$. Scalebar in B = 2 µm.
693
694 **Figure 5: TBI-induced solTNF promotes hippocampal-associated functional impairments.** Sham- or
695 CCI-injured mice, treated with vehicle or XPro1595 (starting 60 minutes post-injury) were assessed on
696 spatial learning and memory in the Morris Water Maze (MWM) for 5 consecutive days (post-injury days
697 7-11). **(A&B)** The vehicle-treated injured mice took significantly longer on day 1 to learn to find the
698 platform, by entering significantly more quadrants. Conversely, XPro1595-treated injured mice were able
699 to find the platform in the same amount of time, entering the same number of quadrants, compared to sham-
700 injured mice (independent of treatment). **(C&D)** Three days after the last training session (14 days post-
701 injury) the mice were assessed on remembering the location of the platform (probe test: platform removed).
702 Mice with TBI spent less time in the platform quadrant than sham-injured mice, and a tendency to enter the
703 platform quadrant less than sham-injured mice. XPro1595-treated injured mice spent an equal amount of
704 time in the platform quadrant compared to sham-injured mice, and an equal amount of entries into the
705 platform quadrant. **(E)** Mice were assessed using the sucrose preference test prior to injury (baseline), and
706 on post-injury days 3, 7 and 14. Prior to injury the mice preferred to drink the 2% sucrose water
707 approximately 90% of the time. Comparatively, vehicle-treated injured mice displayed a temporary
708 reduction in their preference for the sucrose water, which was not observed in the XPro1595-treated injured
709 mice. **(F)** Mice were assessed on their level of hindpaw mechanical hypersensitivity prior to injury
710 (baseline), and on post-injury days 3, 7 and 14. The sham-injured mice displayed a significant increase in
711 hypersensitivity (reduced threshold) 3 days post-injury, that returns to baseline after the first week.

Conversely, the vehicle-treated injured mice display increased hypersensitivity that persists until the end of testing at post-injury day 14. While the XPro1595-treated injured mice display significantly more hypersensitivity 3 days post-injury, this effect is only temporary, similar to the sham-injured mice. Veh = vehicle; XP = XPro1595; (A-D) Sham+Veh n=13, Sham+XP n=12, TBI+Veh n=15, TBI+XP n=14; (E) TBI+Veh n=4, TBI+XP n=5; (F) Sham+Veh n=10, Sham+XP n=11, TBI+Veh n=5, TBI+XP n=4; * = $p<0.05$, ** = $p<0.01$, *** = $P<0.001$.

Figures

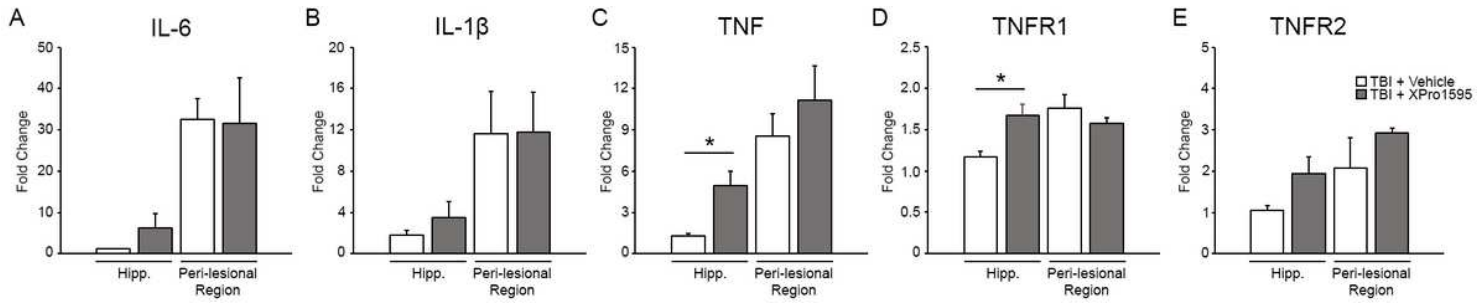

Figure 1

Pro-inflammatory cytokine expression 6 hours following TBI. Graphs show the fold change of expression within the ipsilateral tissue, as compared to the contralateral tissue of IL-6 (A), IL-1β (B), TNF (C), TNFR1 (D), and TNFR2 (E), with either vehicle or XPro1595 treatment. qPCR analysis reveals selective inhibition of soluble TNF does not alter IL-6 or IL-1 β expression. In contract, XPro1595 significantly increased TNF and TNFR1 expression within the hippocampus, with a tendency for increased 660 expression of TNFR2. Hipp=Hippocampal; V=Vehicle; XP=XPro1595; TBI+Veh = white bars; TBI+XP 661 = grey bars; n=4 per group; * p<0.05.

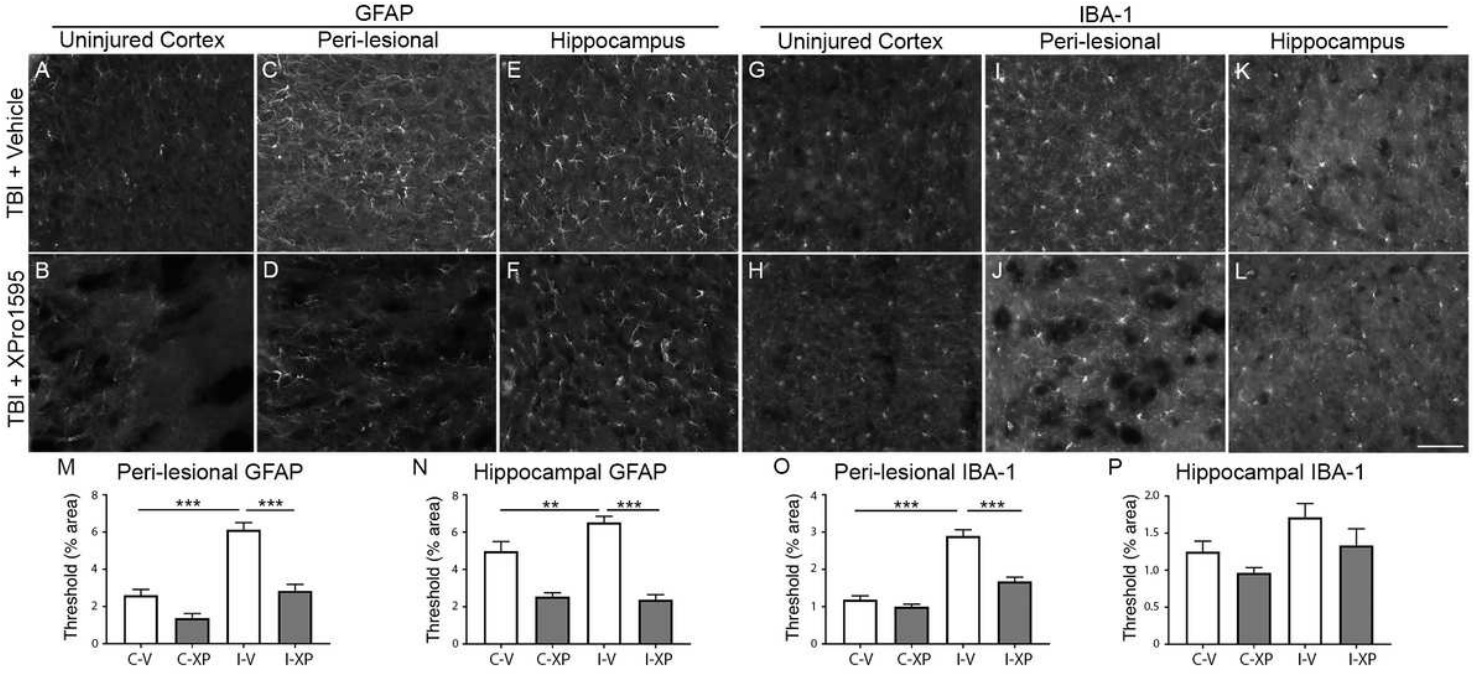

Figure 2

Glial reactivity in the peri-lesional cortex and hippocampus two weeks following TBI. Negligible GFAP (astrocytes) and IBA-1 (microglia/macrophages) protein is expressed in the uninjured cortex (A,B,G&H), and hippocampus (images not shown), independent of treatment. TBI promotes gliosis in both the peri-lesional region and hippocampus (C,E,I&K), although this is prevented by using XPro1595 to neutralize soluble TNF (D, F, J & L). Graphs show semi-quantitation of glial reactivity in the ipsilateral and

contralateral hemisphere following TBI (M-P). C-V = contralateral hemisphere+vehicle; C-XP = contralateral hemisphere+XPro1595; I-V = ipsilateral hemisphere+vehicle; I-XP = ipsilateral hemisphere+ XPro1595; TBI+V n=9, TBI+XP n=9; ** = p<0.01, *** = p<0.001. Scalebar in L = 50 µm.

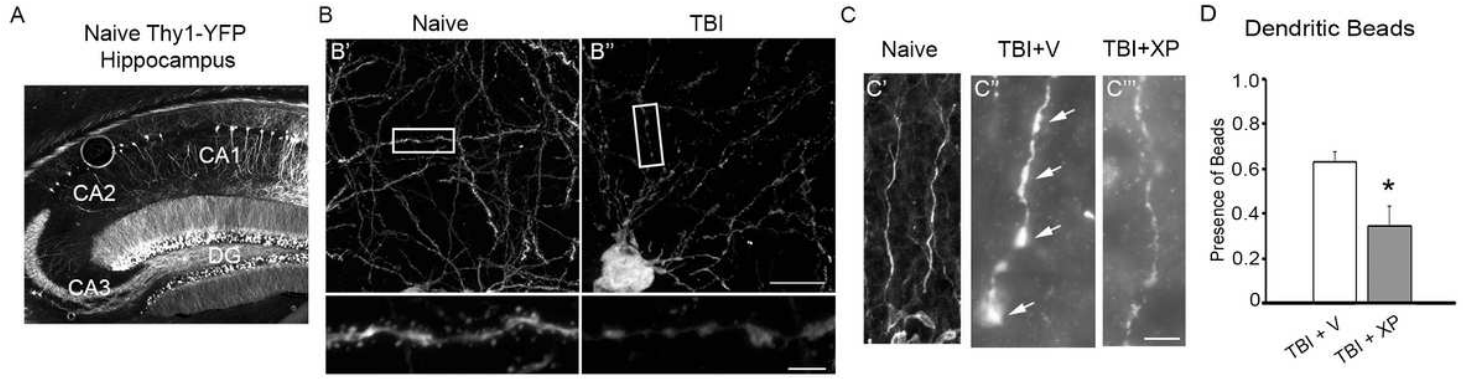

Figure 3

Hippocampal dendritic degeneration following CCI injury. Thy1-YFP-labelled mouse hippocampus showing dentate gyrus (DG), CA1, CA2 and CA3 regions (A). Neuronal dendrites from CA1 region in naive mice show normal morphology (B'), while 3 days post-injury CA1 dendrites develop abnormalities (B"). CCI-injury appears to reduce spine density, and promotes swellings (beading) along the length of the dendrite (B). In naïve uninjured animals, dendrites from immature neurons within the hippocampal DG that are immunoreactive for doublecortin, show an absence of dendritic swellings (C'). However, extensive swellings are observed on immature dendrites of the DG 14 days following the injury (C") that can be significantly reduced when XPro1595 is administered starting 60 minutes post-injury (C""&D). V=Vehicle; XP=XPro1595; TBI+V n=4, TBI+XP n=4; * = p<0.05; Scalebar in B = 20 µm, B inset = 5 µm, and C = 2 µm.

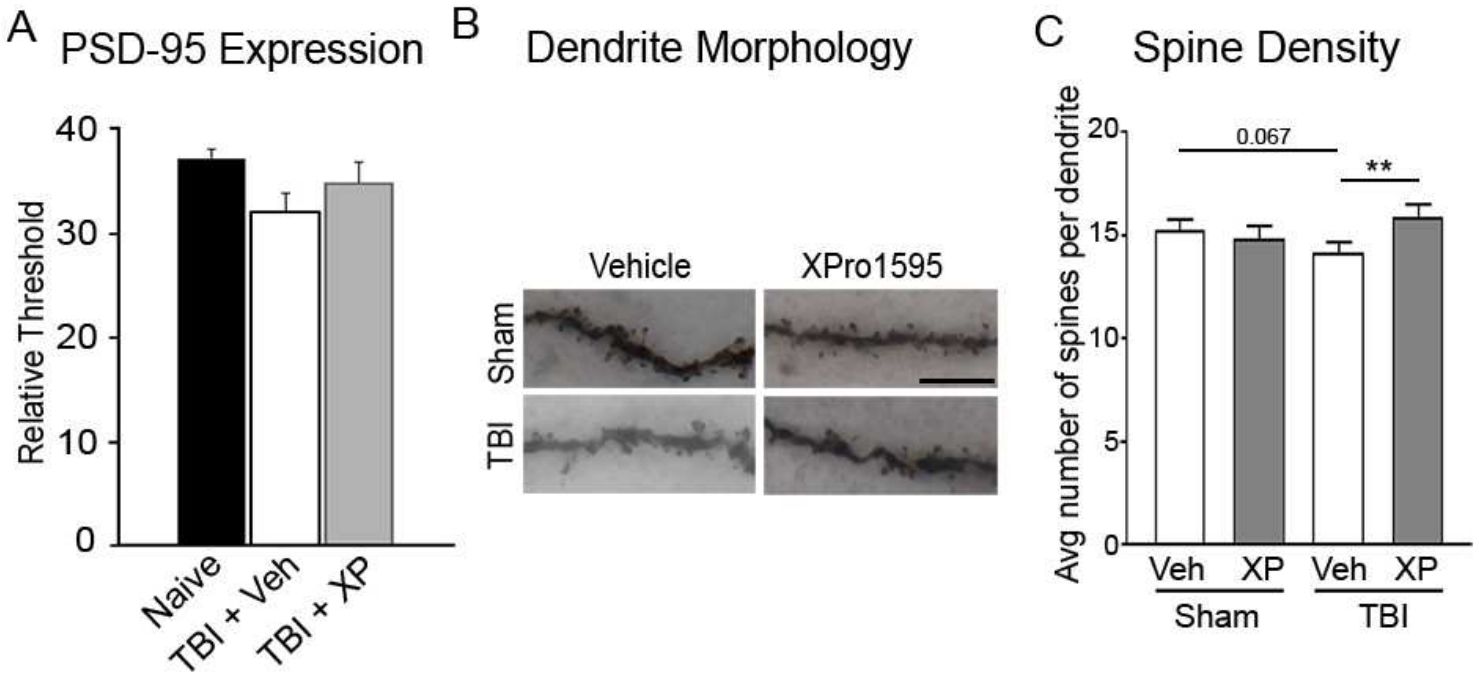

Figure 4

TBI regulates hippocampal dendritic plasticity via soluble TNF activity. The ipsilateral hippocampus was semi-quantitated for PSD-95 expression; a prominent post-synaptic scaffolding protein, 3 days post-CCI injury. Western blot analysis reveals injury reduced hippocampal PSD-95 expression (A), which was prevented in mice treated with XPro1595 one-hour post-injury. (B) Morphology of Golgi-stained hippocampal slices from sham- and CCI-injured mice, treated with either XPro1595 or Vehicle show changes in spine density. Golgi-stained dendrites were quantitated for spine density (number of spines on a dendrite 200 µm in length), revealing that injury reduces dendritic spine density (C), which is prevented in the XPro1595-treated injured mice. Veh=Vehicle, XP=XPro1595; (A) n=3 per group, (C) Sham+Veh n=7, Sham+XP n=5, TBI+Veh n=10, TBI+XP n=10; ** = p<0.01. Scalebar in B = 2 µm.

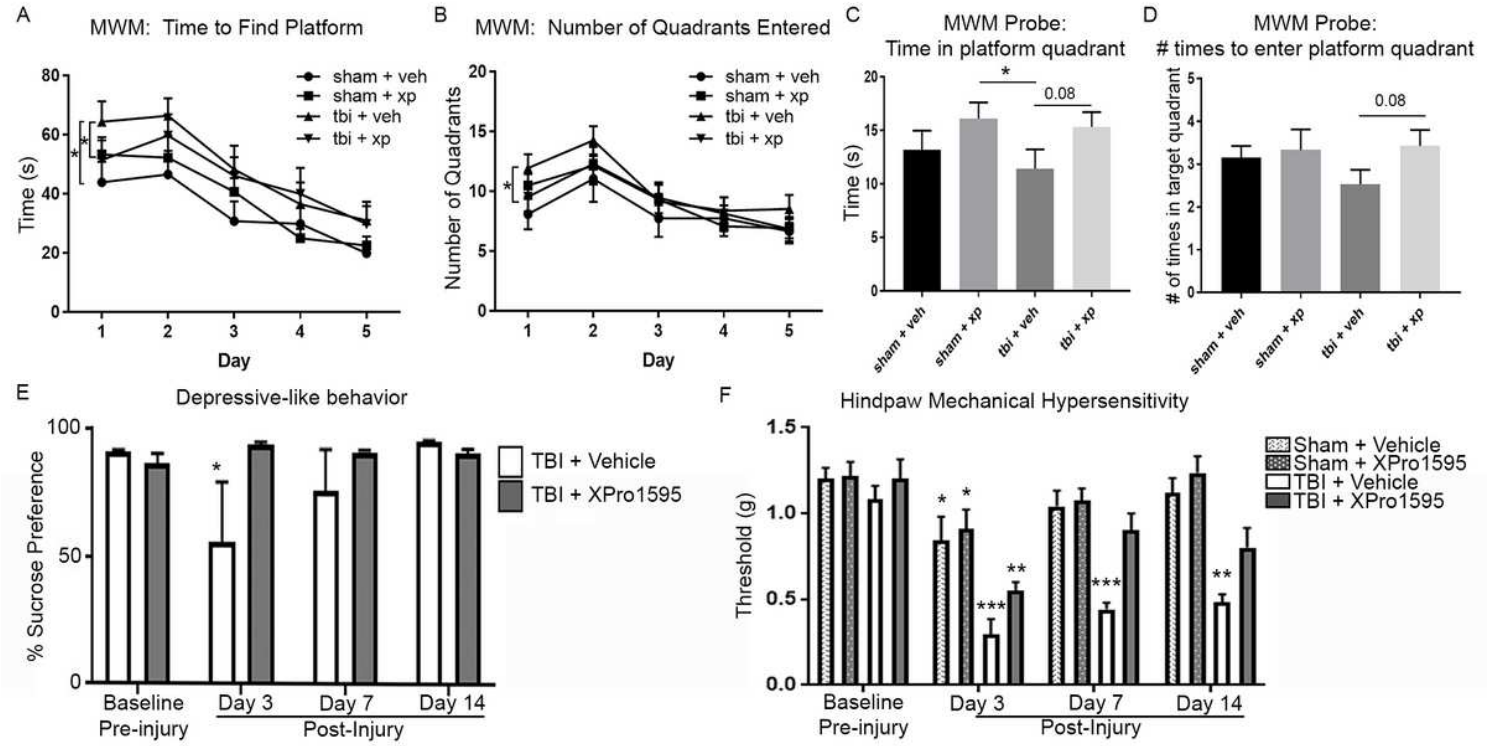

Figure 5

TBI-induced solTNF promotes hippocampal-associated functional impairments. Sham- or CCI-injured mice, treated with vehicle or XPro1595 (starting 60 minutes post-injury) were assessed on spatial learning and memory in the Morris Water Maze (MWM) for 5 consecutive days (post-injury days 7-11). (A&B) The vehicle-treated injured mice took significantly longer on day 1 to learn to find the platform, by entering significantly more quadrants. Conversely, XPro1595-treated injured mice were able to find the platform in the same amount of time, entering the same number of quadrants, compared to sham-injured mice (independent of treatment). (C&D) Three days after the last training session (14 days post-injury) the mice were assessed on remembering the location of the platform (probe test: platform removed). Mice with TBI spent less time in the platform quadrant than sham-injured mice, and a tendency to enter the platform quadrant less than sham-injured mice. XPro1595-treated injured mice spent an equal amount of time in the platform quadrant compared to sham-injured mice, and an equal amount of entries into the platform quadrant. (E) Mice were assessed using the sucrose preference test prior to injury (baseline),

and on post-injury days 3, 7 and 14. Prior to injury the mice preferred to drink the 2% sucrose water approximately 90% of the time. Comparatively, vehicle-treated injured mice displayed a temporary reduction in their preference for the sucrose water, which was not observed in the XPro1595-treated injured mice. (F) Mice were assessed on their level of hindpaw mechanical hypersensitivity prior to injury (baseline), and on post-injury days 3, 7 and 14. The sham-injured mice displayed a significant increase in hypersensitivity (reduced threshold) 3 days post-injury, that returns to baseline after the first week. Conversely, the vehicle-treated injured mice display increased hypersensitivity that persists until the end of testing at post-injury day 14. While the XPro1595-treated injured mice display significantly more hypersensitivity 3 days post-injury, this effect is only temporary, similar to the sham-injured mice. Veh = vehicle; XP = XPro1595; (A-D) Sham+Veh n=13, Sham+XP n=12, TBI+Veh n=15, TBI+XP n=14; (E) TBI+Veh n=4, TBI+XP n=5; (F) Sham+Veh n=10, Sham+XP n=11, TBI+Veh n=5, TBI+XP n=4; * = 716 $p<0.05$, ** = $p<0.01$, *** = $P<0.001$.